Roger E. Stoller[1] and Lawrence R. Greenwood[2]

An Evaluation of Neutron Energy Spectrum Effects in Iron Based on Molecular Dynamics Displacement Cascade Simulations

Presented at 19th International Symposium on the Effects of Radiation on Materials, Seattle, WA, to be submittedfor publication to ASTM.

Research sponsored by the Office of Nuclear Regulatory Research, U.S. Nuclear Regulatory Commission under inter-agency agreement DOE 1886-8109-8L with the U.S. Department of Energy and by the Division of Materials Sciences, U.S. Department of Energy under contract DE-AC05-96OR22464 with Lockheed Martin Energy Research Corp., and the Office of Fusion Energy Sciences, U.S. Department of Energy at the Pacific Northwest National Laboratory.

1. Senior Research Staff, Oak Ridge National Laboratory, P. 0. Box 2008, Oak Ridge, TN 37831-6376
2. Lead Scientist, Pacific Northwest National Laboratory, P. 0 . Box 999, Richland, WA 99352

Roger E. Stoller[1] and Lawrence R. Greenwood[2]

An Evaluation of Neutron Energy Spectrum Effects in Iron Based on Molecular Dynamics Displacement Cascade Simulations

Reference: Stoller, R. E. and Greenwood, L. G., "An Evaluation of Neutron Energy **Spectrum Effects in Iron Based on Molecular Dynamics Displacement Cascade Simulations,"** *Effects of Radiation on Materials, 19th International Symposium, ASTM STP* 1366, M. L. Hamilton, A. S. Kumar, S. T. Rosinski and M. L. Grossbeck, Eds., American Society for Testing and Materials. West Conshohocken, PA, 1999.

Abstract: The results of molecular dynamics (MD) displacement cascade simulations in bcc iron have been used to obtain effective cross sections for two measures of primary damage production: (1) the number of surviving point defects expressed as a fraction of the displacements calculated using the standard secondary displacement model of Norgett, Robinson, and Torrens (NRT). and (2) the fraction of the surviving interstitials contained in clusters that formed during the cascade event. Primary knockon atom spectra for iron obtained from the SPECTER code have been used to weight these MD-based damage production cross sections in order to obtain spectrally-averaged values for several locations in commercial fission reactors and materials test reactors. An evaluation of these results indicates that neutron energy spectrum differences between the various environments do not lead to significant differences between the average primary damage formation parameters. In particular, the defect production cross sections obtained for PWR and BWR neutron spectra were not significantly different. The variation of the defect production cross sections as a function of depth into the reactor pressure vessel wall is used as a sample application of the cross sections. A slight difference between the attenuation behavior of the PWR and BWR was noted; this difference could be explained by a subtle difference in the energy dependence of the neutron spectra. Overall, the simulations support the continued use of dpa as a damage correlation parameter.

1. Senior Research Staff. Oak Ridge National Laboratory, P. 0. Box 2008. Oak Ridge, TN 37831-6376

2. Lead Scientist, Pacific Northwest National Laboratory. P. 0. Box 999, Richland, WA 99352

Keywords: ferritic steels, modeling, molecular dynamics, point defects, pressure vessels, radiation damage, rate theory

Introduction

Radiation-induced embrittlement in reactor pressure vessel (RPV) steels has traditionally been correlated with exposure parameters such as the neutron fluence above 1 MeV or atomic displacements per atom (dpa) [1,2]. One advantage of dpa over fast fluence is that it explicitly accounts for atomic displacements produced by the entire neutron energy spectrum. Therefore, it provides improved correlation when data have been obtained from irradiation facilities with different neutron energy spectra. Differences in neutron energy spectra are manifested as differences in the energy spectra of the primary knockon atoms (PKA) that are produced in elastic collisions with these neutrons. Low energy PKA, such as those produced by thermal neutrons. are somewhat more efficient at net defect production than are high-energy PKA. This suggests that these displacements should be more heavily weighted in dosimetry. Conversely, the lower energy PKA produce fewer point defect clusters that can promote the formation of extended defects that are responsible for mechanical property changes.

The issue of PKA energy effects can be investigated by displacement cascade simulations using the method of molecular dynamics (MD). Although MD simulations can provide a detailed picture of the formation and evolution of displacement cascades, they impose a substantial computational burden. However, recent advances in computing equipment permit the simulation of high energy displacement events involving more than one-million atoms [3-8]; the results presented below will encompass MD cascade simulation energies from near the displacement threshold to as high as 40 keV. These simulations were carried out using the MOLDY code [9], in which the computing time is almost linearly proportional to the number of atoms in the simulation. Higher energy events require a larger atom block as listed in Table 1. Two to three weeks of computer execution time is required to complete the highest energy 40 keV cascade simulations with 1,024,000 atoms for 15 ps on a modem high-speed workstation.

Two parameters have been extracted from the MD simulations: the number of point defects that remain after the displacement event is completed, and the fraction of the surviving interstitials that are contained in clusters. For the purpose of comparison with standard dosimetry, these values have been normalized to the numberofatomic displacements calculated with the secondary displacement model by Norgett, Robinson, and Torrens (NRT) [10]. The energy dependence of the two MD defect parameters was used to evaluate the effects of neutron energy spectrum. Simple, energy-dependent functional fits to the MD results were obtained, and tbe SPECOMP code [11] was used to compute effective cross sections for point defect survival and point defect clustering. PKA spectra for iron obtained from SPECTER [12] were then used to weight these effective cross sections in order to calculate

Table 1: Typical MD cascade parameters and required atom block sizes

Neutron Energy (MeV)	Average PKA Energy (keV)	Corresponding E_{MD} (keV)	NRT Displacements	Atoms in Simulation
0.0034	0.116	0.1	1	3,456
0.0058	0.236	0.2	2	6,750
0.014	0.605	0.5	5	6,750
0.036	1.24	1.0	10	54,000
0.074	2.54	2.0	20	54,000
0.19	6.60	5.0	50	128,000
0.40	13.7	10.	100	250,000
0.83	28.8	20	200	250,000
1.8	61.3	40	400	1,024,000

spectrum-averaged values for various neutron irradiation environments. These include several locations through the wall of RPVs of representative commercial pressurized and boiling water reactors (PWR and BWR), and positions in both water and sodium-cooled materials test reactors.

MD Cascade Simulations

The molecular dynamics code, MOLDY, and the interatomic potential for iron that was used are described in detail in Refs. 9, 13 and 14. Briefly described, the process of conducting a cascade simulation requires two steps. First, a block of atoms of the desired size is thermally equilibrated. This process permits the lattice thermal vibrations (phonon waves) to be established for the simulated temperature, and typically requires a simulation equivalent to approximately IO ps. This atom block can be saved and used as the starting point for several subsequent cascade simulations. Then, the cascade simulations are initiated by giving one of the atoms a defined amount of kinetic energy, E_{MD}, in a specified direction. This atom is equivalent to the PKA following a collision with a neutron. Statistical variability can be introduced by either further equilibration of the starting block or by choosing either a different primary knockon atom or PKA direction. Based on the magnitude of the calculated standard deviations, at least six different cascades are required to obtain statistically representative average parameters at any one cascade energy and temperature.

The MOLDY code describes only elastic collisions between atoms; it does not account for energy loss mechanisms such as electronic excitation and ionization. Thus, the initial energy E_{MD} given to the simulated MD knockon atom is analogous to the damage energy (T_{dam}) in the NRT model [IO]. Using the values of E_{MD} in Table 1, the corresponding E_{PKA} and the NRT defects in iron have been calculated using the procedure described in Ref. IO with the 40 eV displacement threshold recommended in ASTM E521, Standard Practice for Neutron Radiation Damage Simulation by Charged-Particle Irradiation. These values are also listed in Table 1. Note that the difference between the MD simulation, or damage energy, and the PKA energy increases as the PKA energy increases.

The cascade simulations are continued until in-cascade recombination of vacancies and interstitials is complete and the atom block has returned to near thermal equilibrium. The required simulation time varies from about 5 ps for the low-energy cascades to 15-20 ps for the 40 keV cascades at 100 K. Some further point defect recombination and clustering will take place at the longer times associated with point defect diffusion. However, such times are not accessible by the MD method. These results are thereby strictly representative of primary damage formation only. The range of neutron energies covered by these simulations is also listed in Table I and illustrated in Figure 1. The neutron spectra obtained for a typical PWR at the inside of the pressure vessel, and at positions 0.25 (114-T) and 0.75 (3/4-T) of the way through the RPV are shown. MD cascade simulation energies are shown that correspond to atomic recoils from elastic collisions with neutrons of the indicated energies.

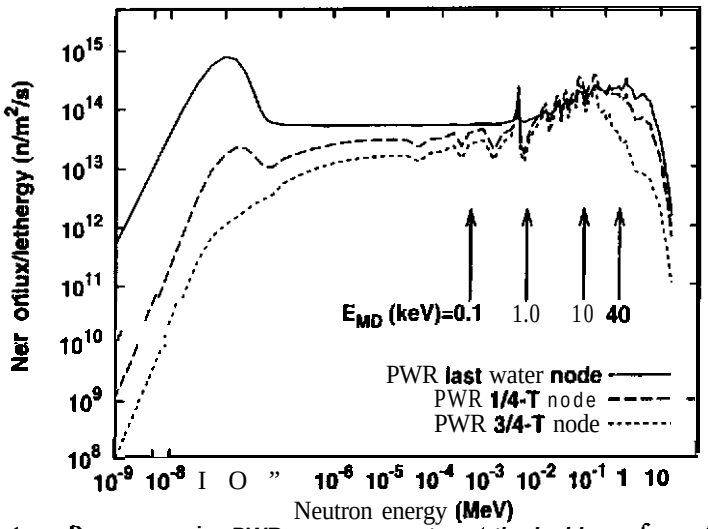

Figure 1 — *Representative PWR neutron spectra at the inside surface of the RPV, and the 1/4-T and 3/4-T RPV locations. Average cascade energies correspond to the indicated neutron energies.*

Two parameters are of primary interest to this work: the number of point defects that survive after in-cascade recombination is complete, and the fraction of the surviving interstitials contained in clusters rather than as isolated defects. The former is important because it is only the surviving point defects that can contribute to radiation-induced microstructural evolution. The latter is significant because these small clusters provide nuclei for the growth of larger defects which can give rise to mechanical property changes. The formation of these small clusters directly within the cascade means that the extended defects can evolve more quickly than if the clusters could only be formed by the much slower process of classical nucleation. For purposes of this work, interstitials were considered clustered if they were within the nearest-neighbor lattice distance of another interstitial. The size distribution of the interstitial clusters produced is a function of the cascade energy [3], and the interstitial clustering fraction is calculated by summing that distribution.

The surviving MD defects can be conveniently described as a fraction of the NRT displacements [IO] and the number of clustered interstitials as a fraction of the surviving MD defects. The energy dependence of the surviving defect fraction (η) and the interstitial clustering fraction (f_{icl}) from the MD simulations is shown in Figures 2 and 3, respectively. Since the MD results did not exhibit a strong dependence on irradiation temperature, all of the results obtained at 100, 600, and 900 K are shown [3-7]. The line drawn through the data in each figure is a nonlinear least-squares fit to the data using the following functions:

$$\eta = 0.5608 \cdot E_{MD}^{-0.3029} + 3.227x10^{-3} \cdot E_{MD} \qquad (1)$$

$$f_{icl} = [0.097 \cdot ln(E_{MD} + 0.9)]^{0.3859} - 7x10^{-6} \cdot E_{MD}^{2.5} \qquad (2)$$

In both Eqns. (I) and (2), the first term in the function dominates the energy dependence up to about 20 keV. The second term accounts for the effect of subcascade formation at the highest energies [5-7]. Mathematically, this term is responsible for the minimum in the defect survival curve and the maximum in the interstitial clustering curve at about 20 keV. As discussed elsewhere [5,6], this change in the energy dependence occurs because subcascade formation makes a single, high energy cascade appear to be the equivalent of several lower energy cascades. Thus, the defect survival fraction is slightly higher, and the interstitial clustering fraction slightly lower at 40 keV than at 20 keV.

The increase in the defect survival fraction between 20 and 40 keV is slight, but it appears to be statistically significant from tbe magnitude of the standard deviations that are shown as error bars in Figure 2. These standard deviations are

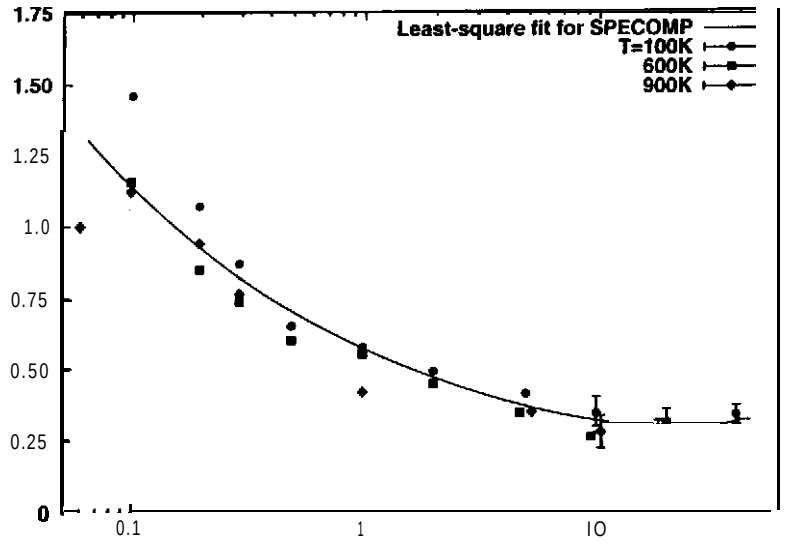

Figure 2 — *Average MD point defect survival fraction as a function of cascade energy; results of MD simulations at 100, 600, and 900K.*

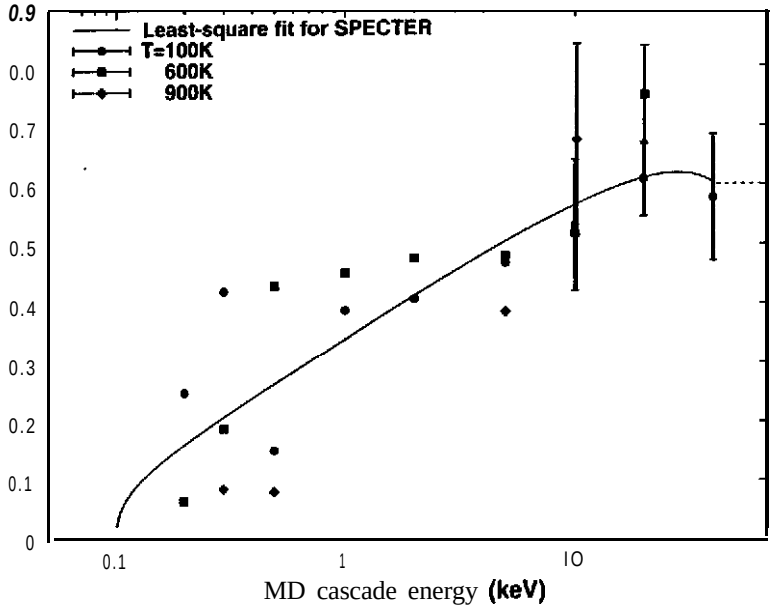

Figure 3 -*Average in-cascade interstitial clustering fraction as a function of cascade energy: results of MD simulations at 100, 600, and 900 K.*

based on the average of 7, 10, and 7 cascades at 10, 20, and 40 keV, respectively. The results of a preliminary analysis of 50 keV cascades is consistent with a slight increase in the cascade survival fraction above 20 keV. However, only four such cascades have been completed at this time and this is too small a number to obtain a reliable average. Additional simulations are underway at 40 and 50 keV to obtain a better statistical estimate of the avenges at each energy. Since the standard deviations on the average interstitial clustering fractions are much larger, the significance of the maximum shown in Figure 3 is less clear. Based on the degree of subcascade formation observed in the 40 keV cascade simulations, it appears unlikely that η and f_{icl} will change significantly at higher cascade energies. 'Therefore. the values calculated from Eqns. (I) and (2) for40 keV were applied for all the higher energy PKA in the SPECOMP and SPECTER calculations.

Defect Production Calculations Using SPECOMP and SPECTER

Energy-dependent defect production cross sections for surviving MD defects and clustered interstitials, and spectrum-averaged values for several irradiation environments were generated by modifying the SPECOMP [I I] and SPECTER [12] computer codes. SPECOMP normally calculates displacement cross sections for compounds using the primary knockon atomic recoil energy distributions contained in a 100-neutron-energy by 100-recoil-energy grid for each of 40 different elements. For the present defect and clustered interstitial calculations, these new functions were used as a factor multiplying the standard displacement cross section equations as a function of the damage energy, T_{dam}. SPECOMP thus produced surviving defect and clustered interstitial cross sections on a 100 point neutron energy grid.

The SPECTER computer code contains libraries of calculated cross sections for displacements, gas production, and total energy distribution, as well as atomic recoil energy distributions for more than 40 elements and various compounds. For a given neutron energy spectrum and irradiation time, the code can be used to calculate the net radiation damage effects, as listed above. In the present case, the SPECOMP calculations for the surviving defect and clustered interstitial cross sections were added to the SPECTER libraries. SPECTER runs for various neutron spectra were then used to produce spectrum-averaged values for the point defect and interstitial clustering fractions.

Results and Discussion

The primary results of these calculations are summarized in Figure 4. The PKA-spectrum-averaged defect survival fraction is shown in Figure 4a, and the interstitial clustering fraction in Figure 4b. In both cases, the effective production cross section has been divided by the NRT dpa cross section. Values are shown for the 114-T and 314-T RPV positions from representative PWR and BWR neutron spectra [15]. Four additional irradiation sites are also shown. These are: positions located in the peripheral target position (PTP) and removable beryllium reflector (RB*) of the High Flux Isotope Reactor (HFIR) at ORNL, and the mid-core and below-core (BC) positions in the Fast Flux Test Facility (FFTF) at the U.S. DOE Hanford Reservation.

Including the HFIR and FFTF positions provides spectra from two broadly

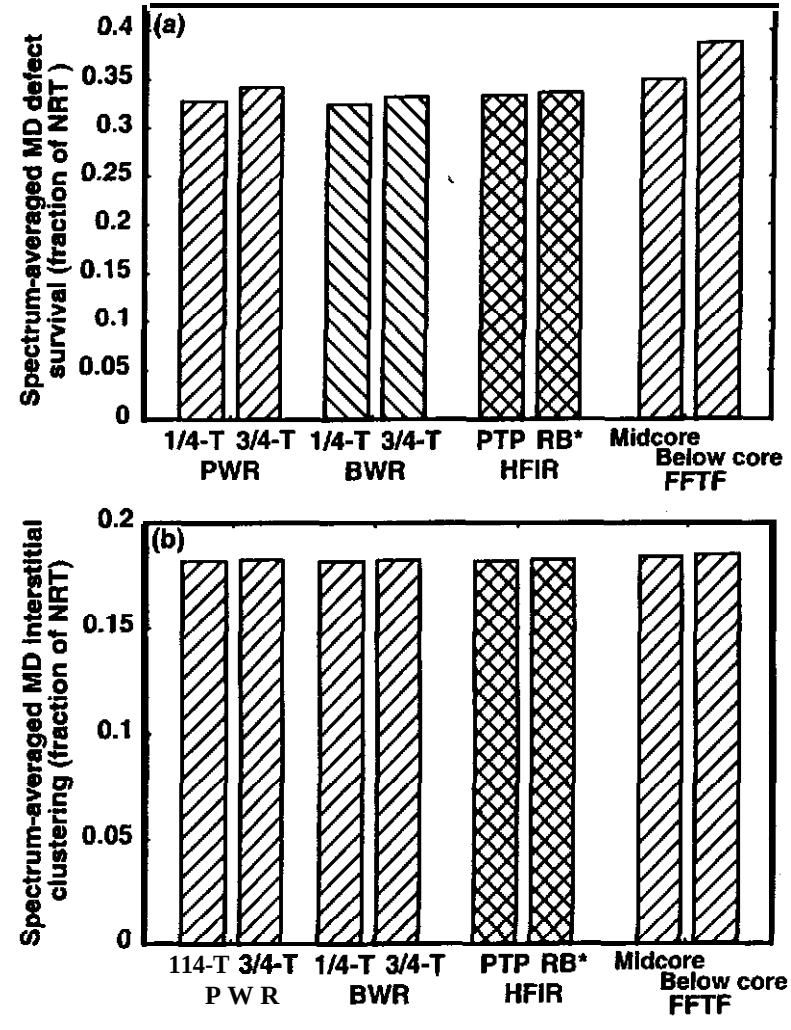

Figure 4 — *Comparison of spectrally-averaged damage production cross sections (per NRT dpa) for various irradiation environments; defect survival ratio is shown in (a) and the interstitial clustering fraction is shown in (b).*

used materials test reactors (although the FFTF is no longer operating). The former is a very high-flux (up to ~10^{19} n/m^2), water-moderated test reactor, and the latter is a liquid metal (Na) cooled fast reactor. In spite of the differences between the various neutron energy spectra, only relatively small differences are observed in the two spectrum-averaged damage cross sections. This is consistent with the observed iron PKA energy distributions shown in Figure 5. In the region where the PKA probability is highest, i.e. for PKA energies between 1 keV and 0. J MeV, the PKA spectra are quite similar.

A slight difference between the PWR and BWR spectra can bc seen in the way the spectra change as a function of thickness through the pressure vessel. This is illustrated in Figure 6, where the spectrum-averaged defect production cross sections are shown for four positions: the last water node point before the RPV, the 1/4 and 3/4 RPV locations, and the first node point in the cavity beyond the RPV. The values for the two reactor types are most similar at the pressure vessel wall, and diverge somewhat at greater depths. The reason for this modest divergence is a subtle difference in the neutron energy spectra and the way in which neutron attenuation occurs. The BWR spectrum is generally considered to be softer than the PWR, and would be expected to give a higher defect survival fraction based on the results shown in Figure 2. However, the average PKA energy at the 1/4-T and deeper positions is actually somewhat higher for the BWR. This can be rationalized by a comparison of the 114-T neutron spectra in Figure 7, where the energy-dependent group fluxes are normalized using their respective peak values. The BWR spectrum shows both a higher relative thermal flux and a higher relative fast flux than the PWR spectrum. Since most of the displacements are generated by the higher energy neutrons, the effective avenge PKA energy for the BWR spectrum is greater than that of the PWR. Although the details of this comparison may apply only to these particular reference spectra [15], it illustrates how using a dose or correlation parameter that makes use of the complete neutron spectrum can provide more information than is obtained when only a simple fluence greater than a specified energy threshold is used.

The projected attenuation of the damage rate through a PWR reactor pressure vessel is shown in Figure 8, in which results based on the MD-based damage cross sections are compared to neutron fluence (E>1.0 MeV) and dpa. The results are normalized to the value obtained at the first node of the transport calculation inside the RPV. The other four points plotted are the 1/4-T, 3/4-T, the last node in the RPV, and the first node in the reactor cavity. Because an increasing fraction of displacements are caused by lower energy neutrons as the high energy end of the spectrum is lost, dpa is attenuated more slowly than fast fluence. The MD point defect survival is attenuated somewhat more slowly than dpa because of the increased survival fraction at lower energies shown in Figure 2. However, the small difference between dpa and the MD-based results shown in this figure indicates that

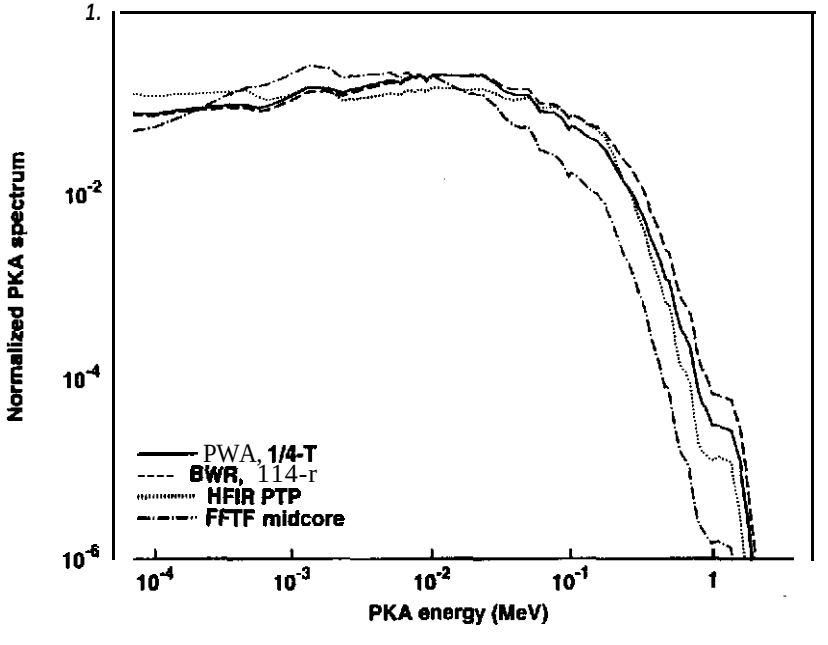

Figure
1/4-T

id BWR

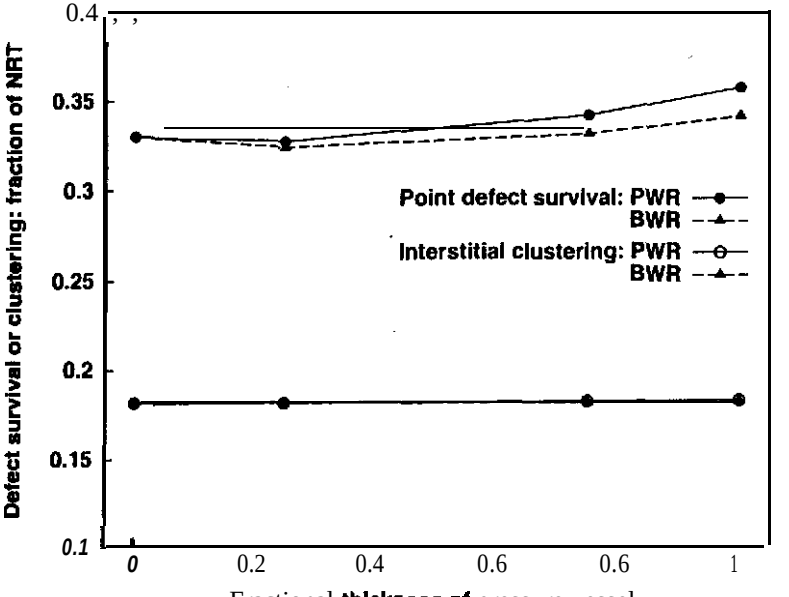

Figure *6 — Variation of spectrally-averaged damage production cross sections (per NRT dpa) through the RPV for PWR and BWR.*

dpa accounts for nearly all of the spectral shift associated with attenuation through the RPV.

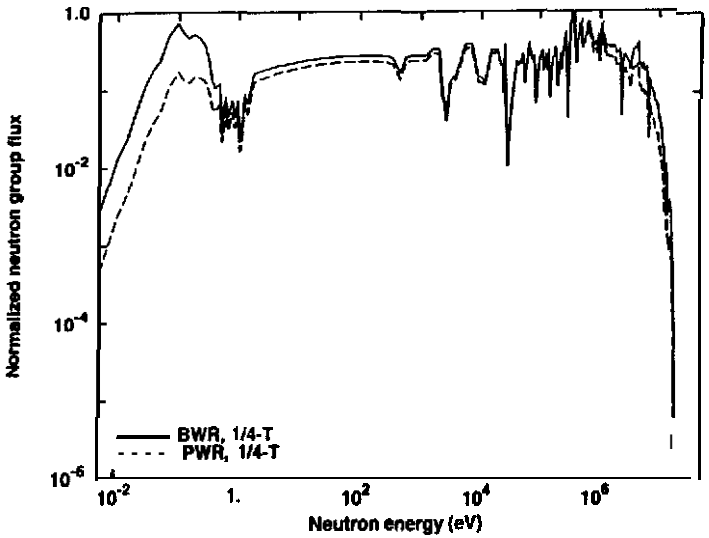

Figure 7 -*Normalized neutron spectra for PWR and BWR at the 1/4-T location. Note that the BWR fluxes are higher of both the lowest and highest energies.*

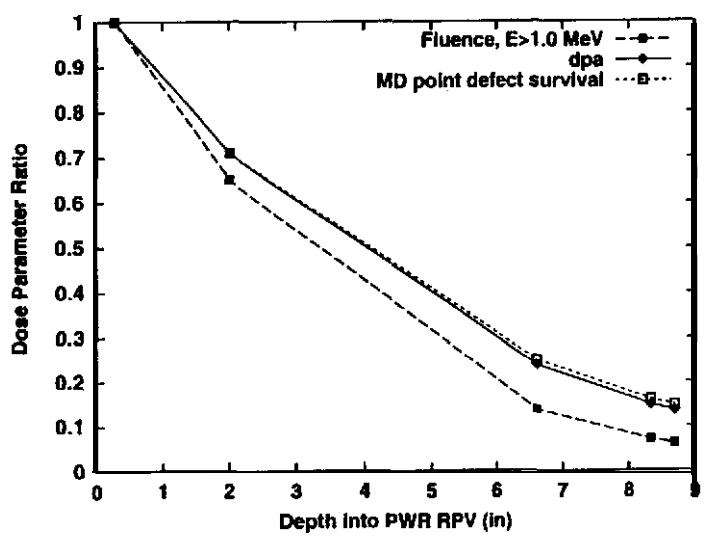

Figure 8 -*Attenuation of fast neutron fluence, dpa, and MD-basedpoint defect survival fraction through the wall of PWR reactor pressure vessel.*

Summary

Although it is not yet possible to simulate the highest energy displacement cascades generated in the materials used in fission reactors, the analysis of MD cascade simulations in bcc iron for energies up to 40 keV are of considerable relevance. For example, while Fig. 5 indicates that there is a significant probability of PKA production at energies above 100 keV for fission reactor neutron spectra, the highest average PKA energy obtained from SPECTER for any of the LWR RPV neutron spectra was only 23 keV.

The primary damage parameters derived from the MD results exhibit a strong dependence on cascade energy up to about JO keV. At this point, a high degree of subcascade formation leads to nearly asymptotic behavior at higher cascade energies. However, there is also evidence of a minimum in the fractional defect survival curve at -20 keV. This potential for a slight increase in the cascade survival fraction above 20 keV is being investigated further. Analysis of cascade and subcascade morphology indicates that the primary damage parameters will not significantly change at higher energies, which implies that the results reported here should be relevant to an evaluation of neutron energy spectrum effects.

Notably, the spectrum-averaged defect production cross sections calculated for several fission reactor neutron spectra were all quite similar. This included locations within the pressure vessels of commercial PWRs and BWRs, as well as locations in light water and liquid metal cooled materials test reactors. Since the cross sections were so similar, it appears unlikely that spectral differences will significantly influence comparisons of PWR and BWR data when dpa is used as a correlation parameter. In addition, an evaluation of damage attenuation through the RPV wall for both reactor types indicates that the spectrum-avenged, MD-based damage production cross sections are attenuated at a rate which is not significantly different from the dpa cross section. This implies that neutron energy spectrum changes due to attenuation should also be well accounted for through the use of dpa.

Finally, the spectrum-averaged defect production cross sections obtained from the MD results can be used to guide the selection of appropriate radiation damage source terms in the kinetic models used to investigate. radiation-induced microstructural evolution and embrittlement in pressure vessel steels. It has not been demonstrated that these results are relevant to materials other than ferritic steels; however, a comparison of MD cascades in fcc copper and bcc iron up to IO keV revealed many similarities between these two materials [3].

Acknowledgments

Research sponsored by the Office of Nuclear Regulatory Research, U.S. Nuclear Regulatory Commission under inter-agency agreement DOE 1886-8109-

8L with the U.S. Department of Energy and by the Division of Materials Sciences, U.S. Depanment of Energy under contract DE-AC05-96OR22464 with Lockheed Martin Energy Research Corp., and the Office of Fusion Energy Sciences, U.S. Department of *Energy* at the Pacific *Northwest National* Laboratory.

References

[1] R. E. Stoller and G. R. Odette, *Journal of Nuclear Materials* 186 (1992) 203-205.

[2] Recommendations of IAEA Specialists Meeting on Radiation Damage Units in Graphite and Ferritic and Austenitic Steels, Nuclear *Engineering and Design 33* (1975) 48.

[3] W. J. Phythian, R. E. Stoller, A. J. E. Foreman, A. F. Calder, and D. J. Bacon, *Journal of* Nuclear *Materials* 223 (1995) 245-261.

[4] R. E. Stoller, Journal *of Nuclear Materials* 233-237 (1996) 999-1003.

[5] R. E. Stoller, *JOM* (formerly *Journal of Metals)* 48 (19%) 23-27.

[6] R. E. Stoller, G. R. Odette. and B. D. Wirth, Journal *of Nuclear Materials* 251 (1997) 49-69.

[7] R. E. Stoller, "Molecular Dynamics Simulations of High Energy Cascades in Iron," Microstructure of Irradiated Materials, I. M. Robertson, L. E. Rehn, S. J. Zinkle, and W. J. Phythian, Editors, Materials Research Society, Pittsburgh, PA, 1995. pp. 21-26.

[8] R. E. Stoller and *L. R.* Greenwood," *Journal of Nuclear Materials* 271&272 (1999) 57-62.

[9] M. W. Finnis, "MOLDY6-A Molecular Dynamics Program for Simulation of Pure Metals:' AERE R-13182, UK AEA Harwell Laboratory (1988).

[10] M. J. Norgett, M. T. Robinson. and I. M. Torrens, *Nuclear Engineering and Design 33* (1975) 50-54.

[11] L. R. Greenwood, "SPECOMP Calculations of Radiation Damage in Compounds," Reactor Dosimetry: Methods, Applications, and Standardization, ASTM STP 1001, H. Farrar IV and E. P. Lippincott, Eds., American Society of Testing and Materials. West Conshohocken, PA, 1989, pp. 598-602.

[12] L. R. Greenwood and R. K. Smither, "SPECTER: Neutron Damage Calculations for Materials Irradiations," ANL/FPP/TM-197, Argonne National Laboratory, Argonne, IL, January 1985.

[13] M. W. Finnis and J. E. Sinclair, *Philosophical Magazine* A50 (1984) 45-55 and Erratum, *Philosophical Magazine A53 (1986)* 161.

[14] A. F. Calder and D. J. Bacon, *Journal of Nuclear Materials 207 (1993)* 25-45.

[15] T.E. Albert, M.L. Gritzner, G.L. Simmons, and E.A. Straker, "PWR and BWR Radiation Environments for Radiation Damage Studies. "EPRI NP-152, Electric Power Research Institute, Palo Alto, CA, September 1977.